

**Low level viral persistence
after infection with LCMV:
a quantitative insight through
numerical bifurcation analysis**

*Tatyana Luzyanina, Koen Engelborghs, Stephan Ehl,
Paul Klenerman, Gennady Bocharov*

Report TW 321, March 2001



Katholieke Universiteit Leuven
Department of Computer Science
Celestijnenlaan 200A – B-3001 Heverlee (Belgium)

Low level viral persistence after infection with LCMV: a quantitative insight through numerical bifurcation analysis

*Tatyana Luzyanina**, *Koen Engelborghs†*, *Stephan Ehlf‡*,
Paul Klenerman§, *Gennady Bocharov¶*

Report TW 321, March 2001

Department of Computer Science, K.U.Leuven

Abstract

Many important viruses persist at very low levels in the body in the face of host immunity, and may influence the maintenance of this state of immunity. To analyse low level viral persistence or state of "infection immunity" in quantitative terms, we use a mathematical model of antiviral cytotoxic T lymphocyte (CTL) response to lymphocytic choriomeningitis virus (LCMV). This model is described by a nonlinear system of delay differential equations (DDEs). The model predictions related to coexistence of virus and CTL populations are obtained using recently developed numerical bifurcation analysis techniques for DDEs. Domains where low level LCMV coexistence with CTL memory is possible, either as an equilibrium state or an oscillatory pattern, are identified in spaces of the model parameters characterising the interaction between virus and CTL populations. In the "memory" phase, i.e. after acute infection has been controlled, these include the rate constants of virus growth, precursor and effector CTL death, activation and differentiation of precursor CTL and CTL-mediated virus elimination. Our analysis suggests that the coexistence of replication competent virus below the conventional detection limit (of about 100 pfu per spleen) in the immune host as an equilibrium state requires the per day relative growth rate of the virus population to decrease at least 5 fold compared to the acute phase of infection. Oscillatory patterns in the dynamics of persisting LCMV and CTL memory, with virus population varying between 1 to 100 pfu per spleen, are possible within quite narrow intervals of the rates of virus growth and precursor CTL population death. This is due to a high sensitivity of the amplitude of oscillations to changes in the parameters. These observations may be relevant to low level viral persistence and CTL memory in human infections such as HBV, HCV and, probably, HIV.

Keywords : viral persistence, CTL memory, mathematical model, numerical bifurcation analysis.

AMS(MOS) Classification : Primary : 92C50, Secondary : 34K99.

*Department of Computer Science, K.U.Leuven, Celestijnenlaan 200A, B-3001, Leuven, Belgium. On leave from IMPB, RAS, Pushchino, Moscow region, 142292, Russia.

†Department of Computer Science, K.U.Leuven, Celestijnenlaan 200A, B-3001, Leuven, Belgium.

‡Children's Hospital, University of Freiburg, Mathildenstr. 1, D-79106, Freiburg, Germany.

§Nuffield Department of Clinical Medicine, Level 7, John Radcliffe Hospital, Oxford University, Oxford OX3 9DU, UK.

¶Department of Infectious Disease Epidemiology, Imperial College School of Medicine, St. Mary's Campus, Norfolk Place, London W2 1PG, UK. On leave from the Institute of Numerical Mathematics, RAS, Moscow, 117991, Russia.

1 Introduction

Interaction between pathogens and their hosts is the focus of current research in immunology since viral infections caused by, e.g. HIV-1, hepatitis B virus (HBV) and hepatitis C virus (HCV) present major health problems. Among other factors, the outcome of the pathogen-host interaction depends on what has been discussed as a "*numbers game*" between the infecting virus and the immune system [10, 58, 59] and ranges from elimination of the virus below *detection levels* paralleled by establishment of immunological memory to the chronic high level persistence with suppression of specific immune responses. Understanding the relationships between various types of infection dynamics and the parameters of the '*players*', which determine the various outcomes, is of fundamental importance for viral immunology.

There is increasing experimental evidence supporting the view that non- or low-cytopathic types of infections (LCMV, HBV, HCV, HIV) are never completely eliminated to a sterile state from the infected hosts but are controlled by *infection-immunity* [58]. "Infection-immunity" refers to a state of stable coexistence of continuing immunity together with *low level infection*, so that immunological memory can be interpreted as the continuous restimulation of a low level response. The factors which influence the maintenance and composition of immunological memory over long periods of time remains largely unknown [1, 20].

Virus-specific CD8⁺ cytotoxic T lymphocyte (CTL) responses represent a major immune mechanism of protection against many viral infections through the killing of virus-infected cells and secretion of antiviral factors. Primary infection normally leads to CTL dynamics that has three distinctive phases: clonal expansion, contraction and memory persistence [1]. The CTL population during the memory phase is heterogeneous with respect to the activation state (resting-, cycling- or effector cells) and the life-span of the cells [12, 13, 45, 46, 52, 55]. The quantitative composition and the protective function of the CTL memory population strongly depend on continuous stimulation coming from persisting antigen and/or bystander signals. The type of memory elicited, its long-term maintenance and protective efficacy essentially depend on the virus and the persistence of viral antigens in the host [38, 39]. Some viruses do not persist as intact highly replicative virus in the host but rather as attenuated virus forms [3, 57].

The experimental system based on murine lymphocytic choriomeningitis virus (LCMV) infection is a generally accepted and widely used model to examine the role of virus and host parameters in various types of infection outcomes [25, 58]. LCMV is non-cytopathic and CTLs are responsible for both the initial control of the virus and immunopathology. This experimental model has been proved to be very instructive in understanding the role of antigen in the generation and maintenance of T cell memory [13, 26, 35, 38, 39]. It has been shown that the memory population of LCMV-specific CTL can persist at elevated numbers in the absence of antigen [34, 36]. However, the functional properties of the memory pool, in particular its ability to protect against peripheral infection with LCMV rapidly, depend on the persistence of viral antigen which appears to keep a certain fraction of CTL memory population in the activated effector state [13, 60]. The duration of protective immunity was shown to be related to the persistence of antigen in the LCMV system [26, 39]. It has been experimentally proved that LCMV can persist for some time at very low levels (below detection by conventional assays) in immune mice [9, 24, 38, 42, 54] and the duration of persistence of antigen depends on the way the antigen is delivered to the host [38].

Quantitative parameters of low level LCMV coexistence with CTL memory (such as replication rate and viral population density) are difficult to assess experimentally because of methodological limitations of existing analytical techniques. Interaction of the LCMV with the host's immune responses represents a complex nonlinear system that requires application of mathematical modelling in order to develop a quantitative insight into the kinetic mechanisms underlying various patterns of the population dynamics of the viruses and cells. Recently, a number of mathematical models have been proposed to examine the phenomenon of exhaustion of virus-specific CTL responses observed in high-viral load infections or in immune-deficient hosts [7, 22, 47, 53]. Although these models differ somewhat in their assumptions, they all "generate" a bell-shaped dose-response function for virus-induced CTL proliferation, i.e. high viral loads lead to suppression of immune responses.

In the present study we consider a mathematical model of antiviral cytotoxic T cell responses [7] to examine in detail the quantitative characteristics of low level LCMV persistence. This model has been previously used to analyse the impact of the initial number of precursor CTL on the outcome of LCMV infection [14], the population structure and function of LCMV-specific CTL memory resulting from bystander and antigen-specific stimulation [8], and the rate of virus clearance in the acute phase of LCMV infection [6]. The minimal number of precursor CTLs required for protection of C57BL/6 mice against high viral load persistence after infection with 1 pfu of LCMV-Docile was predicted (protection unit) using the same model [14].

Here we use this model to address the following questions: *(i)* what are the necessary conditions in terms of the turnover rates for virus and memory CTLs for low level virus persistence in immune mice; *(ii)* what are the effects of virus and CTL parameters on the stability and the level of virus persistence; *(iii)* how does the composition of CTL population in the memory phase depend on the level of virus persistence; *(iv)* are oscillatory patterns in viral and CTL dynamics during the memory phase possible? The above issues are answered through numerical bifurcation analysis of the model using the recently developed software package DDE-BIFTOOL [15]. Namely, we study steady states (equilibria) and periodic solutions (periodic oscillations) of the model, their stability features and bifurcations through varying the virus and immune system parameters within certain ranges characteristic of the T cell memory persistence. LCMV infection is used here as a fundamental experimental reference system where detailed quantitative information is available so that the mathematical predictions allow direct interpretation and comparison with experimental data to be made.

The remainder of this paper is structured as follows. In Section 2 we describe briefly the LCMV infection model. In Section 3 we characterise the memory phase of immune mice and present existing experimental knowledge. Numerical methods and their application to the model under study are described in Section 4. Section 5 presents bifurcation analysis of the model related to coexistence of a low level viral population and memory CTL. We discuss the obtained results in Section 6. Section 7 contains conclusions.

2 Mathematical model

The mathematical model of antiviral CTL response developed previously [7] is based upon assumptions reflecting general mechanisms of virus-host interaction: *(i)* virus-specific CTLs

are primarily responsible for control of infection with non-cytopathic viruses; *(ii)* the virus population stimulates clonal expansion and differentiation of the specific CTL precursors (CTLp) into effector cells; *(iii)* a high viral load leads eventually to inhibition of CTL responses via anergy and activation-induced cell death by apoptosis; *(iv)* in the absence of viral antigens the homeostasis of naive CTLs reflects a balance between the input of the precursor CTLs from thymus and their death at the periphery; *(v)* virus replication in the host exhibits a logistic-type growth, whereas the elimination follows a second-order kinetics. These processes define the structure of a system of delay differential equations describing the rates of change of the population densities of virus, $V(t)$, precursor CTL, $E_p(t)$, effector CTL, $E_e(t)$, and the cumulative viral load, $W(t)$,

$$\begin{cases} \frac{d}{dt}V(t) = \beta V(t)\left(1 - \frac{V(t)}{V_{mvc}}\right) - \gamma_{VE}E_e(t)V(t), \\ \frac{d}{dt}E_p(t) = \alpha_{E_p}(E_p^0 - E_p(t)) + \frac{b_p}{(1+W(t)/\theta_p)^2}V(t-\tau)E_p(t-\tau) - \alpha_{AP}V(t-\tau_A)V(t)E_p(t), \\ \frac{d}{dt}E_e(t) = \frac{b_d}{(1+W(t)/\theta_E)^2}V(t-\tau)E_p(t-\tau) - b_{EV}V(t)E_e(t) - \alpha_{AE}V(t-\tau_A)V(t)E_e(t) \\ \quad - \alpha_{E_e}E_e(t), \\ \frac{d}{dt}W(t) = b_WV(t) - \alpha_WW(t). \end{cases} \quad (1)$$

In the equation for $V(t)$, the first term on the right-hand side describes the virus growth with an upper limit V_{mvc} due to the limited amount of sensitive tissue cells supporting virus replication, and the second term takes into account the clearance of viruses due to lysis of the virus-infected cells by effector CTLs.

In the equation for $E_p(t)$, the first term describes the maintenance of virus-specific precursor CTL at a certain level through their export from thymus and death in the periphery. The second term accounts for an increase in the number of CTL precursors resulting from virus-induced proliferation with the inhibitory effect of cumulative virus load on clonal expansion. The last term describes activation induced cell death by apoptosis.

The dynamics of $E_e(t)$ is determined by the appearance of mature effector CTLs due to the division and differentiation of antigen-stimulated precursor CTLs with the down-regulation of the differentiation process of CTLp due to high virus antigen load (the first term); the decrease in the number of effector CTLs as a consequence of lytic interactions with virus-infected target cells (the second term); the activation-induced cell death of effector CTLs and natural death of effector CTL due to their finite life span (two last terms).

In the equation for $W(t)$, the first term describes the increase in the total viral antigen load due to virus spread in the host and the second one accounts for the decrease of the inhibitory effect of high virus loads on the virus-specific CTLs as the virus is eliminated.

The initial estimates for the parameters of the model were obtained from various experimental sources (see [7] for details) and further refined by fitting to homogeneous data sets representing the dynamics of virus load and CTL responses during primary LCMV-Docile infection of C57BL/6 mice, i.e. during the clonal expansion and contraction phases [33]. The whole set of model parameters is given in Table 1.

We use model (1) to study the coexistence of a low level viral population with a high number of virus-specific CTLs during the memory phase of immune response. The scheme depicted in

Fig. 1 shows qualitatively the within host dynamics of virus and CTL populations from primary infection into the memory phase.

Parameter	Biological meaning	Units	Best-fit estimate
β	Replication rate constant of viruses	1/day	3.35
γ_{VE}	Rate constant of virus clearance due to effector CTLs	ml/(cell day)	$1.34 \cdot 10^{-6}$
V_{mvc}	Maximal virus concentration in spleen	particles/ml	$4.82 \cdot 10^7$
τ	Duration of CTL division cycle	day	0.6
b_p	Rate constant of CTL stimulation	ml/(particle day)	$7.73 \cdot 10^{-5}$
b_d	Rate constant of CTL differentiation	ml/(particle day)	$7.73 \cdot 10^{-4}$
θ_p	Virus load threshold for anergy induction in precursor CTLs (proliferation process)	particle/ml	$3.25 \cdot 10^6$
θ_E	Virus load threshold for anergy induction in effector CTLs (differentiation process)	particle/ml	$3 \cdot 10^5$
b_{EV}	Rate constant of effector CTL death due to lytic interactions with virus-infected cells	ml/(particle day)	0
α_{E_p}	Rate constant of natural death for precursor CTLs	1/day	0.542
α_{E_e}	Rate constant of natural death for effector CTLs	1/day	0.01
E_p^0	Homeostatic concentration of LCMV-specific CTLs in spleen of unprimed mouse	cell/ml	265
τ_A	Duration of commitment of CTLs for apoptosis	day	5.6
α_{AP}	Rate constant of apoptosis for precursor CTLs	(ml/particle) ² /day	$7.5 \cdot 10^{-16}$
α_{AE}	Rate constant of apoptosis for effector CTLs	(ml/particle) ² /day	$4.36 \cdot 10^{-14}$
b_W	Rate constant of viral load increase	1/day	1
α_W	Rate constant of restoration from the inhibitory effect of virus load	1/day	0.11

Table 1: List of the model parameters.

3 CD8⁺ T lymphocyte memory

Transition of the LCMV-specific CD8⁺T cell responses from the acute to the memory phase is associated with *a major change* of quantitative parameters characterising the virus and CTL population dynamics. CTLs have a finite life-span at the single cell level. This implies that there should be mechanisms of memory maintenance that help to counter a gradual attrition of the memory pool [12, 20]. Both bystander and virus antigen-specific stimuli contribute to the proliferation, differentiation and death of CTL during the memory persistence phase affecting the cellular composition and functional properties of the CTL memory pool (see analysis in [8]). Therefore, the population life-spans of CTL subsets (represented in the model by $\alpha_{E_p}, \alpha_{E_e}$) in the memory phase depend on many processes including the CD4⁺ T cell help, B cell function, expression of survival factors such as Bcl-2 or apoptosis-inducing cytokines like FasL or TNF molecules, etc. [21, 28, 31]. Generally, on a per cell basis memory CD8⁺ T cells are primed for effector functions (b_d) and can be activated for proliferation (b_p) by lower concentrations of antigen and all types of APCs compared to “naive” CTL [20, 41, 48]. However, in CD4⁺ T cell deficient mice the dynamics of CTL memory is associated with decreased proliferation and differentiation rates (b_p, b_d), so that finally the virus reappears above the detection level,

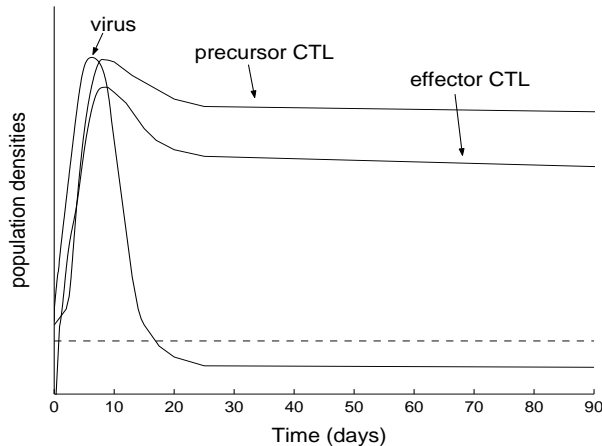


Figure 1: Scheme of the within host dynamics of virus and two CTL populations after primary infection: the expansion (increase in CTL number), contraction (decline in CTL number after the peak of response) phases and the memory phase (a high level of persisting CTLs). A logarithmic scale is used for population densities. The dashed line denotes the detection limit of the virus in experiments.

CTL-mediated control fails and high viral load chronic infection is established [42, 50]. Although memory CTLs have lower activation thresholds, the progression through the cell cycle of activated CTL in the memory phase can take a long time (represented by τ) compared to the acute infection [55].

CTL memory, determined by initial clonal burst size, is heterogeneous in terms of the cell activation status and represents low level responses driven by various stimuli [1, 20, 56, 58]. Recent experimental evidence indicates that (i) after acute infection with LCMV the virus might persist for some time in spleen cells at a frequency of 1 copy per 10^4 to 10^5 splenocytes, giving an estimate of about 500 to 5000 DNA copies per spleen [24]; (ii) a difference in total LCMV RNA copies between the peak of infection ($10^8 - 10^9$ copies per spleen) and the memory phase (10^3 or fewer copies per spleen) has been observed (Klenerman, unpublished observations); (iii) infectious LCMV may persist at no more than 10^2 pfu per spleen [9] and in some cases at the level of 10^3 pfu per kidney [54].

How can the virus population persist in the face of CTL memory? There is a diverse array of biological mechanisms that are used by viruses to escape complete elimination by the immune system, ranging from those based on a limited growth, cell-to-cell passage without maturation, localisation in an immunologically privileged site and integration into the host cell chromosome to those based on decreasing immune detection and destruction, e.g. via down-regulation of MHC-restricted antigen presentation [3, 40, 51]. In terms of kinetics the implication is that the replication rate and CTL-mediated elimination rate of LCMV (represented by β and γ_{VE} , respectively) might well be reduced during transition from the acute to the low level persistence phase. Indeed, available data on the growth kinetics of LCMV after immune therapy of a persistent viral infection [2] or in $CD4^+$ T cell or B cell-deficient mice [42] show a much lower rate of viral growth compared to the acute infection.

Using the above listed factors we specify plausible ranges of the model parameters relevant for virus and CTL persistence during the memory phase, see Table 2. The last column of this

table gives the corresponding references they are based on. We investigate coexistence of the viral and CTL populations in the memory phase through numerical bifurcation analysis of the virus-host interaction model (1). The *critical effects* of various combinations of viral and CTL parameters on this coexistence are examined with particular focus on low level viral persistence.

Parameter	Biological meaning	Units	Range	References
α_{E_p}	Rate constant of natural death for precursor CTLs	1/day	0.001 – 0.5	[1, 11, 20, 21, 26]
α_{E_e}	Rate constant of natural death for effector CTLs	1/day	0.1 – 0.4	[28, 31, 34, 36, 46]
β	Replication rate constant of viruses	1/day	< 5	[2, 32, 33, 42]
b_p	Rate constant of CTL stimulation	ml/(particle day)	$10^{-5} - 10^{-3}$	[20, 41, 48]
b_d	Rate constant of CTL differentiation	ml/(particle day)	$10^{-4} - 10^{-2}$	[20, 41, 48]
γ_{VE}	Rate constant of virus clearance due to effector CTLs	ml/(cell day)	$10^{-7} - 1.34 \cdot 10^{-6}$	[40, 51]
τ	Duration of CTL division cycle	day	0.4 – 2	[52, 55]

Table 2: Admissible ranges of the model parameters related to the virus and CTL persistence in the memory phase and estimated from data presented in the indicated references.

4 Numerical techniques

In the context of dynamical system analysis, the coexistence of a low level viral population and CTL memory corresponds to a stable steady state solution (equilibrium) or to a stable periodic solution (i.e. oscillatory solution repeating itself after a finite time) of model (1) with V , respectively $V(t)$, below a (small) value, e.g. below the detection limit of the virus in experiments. Model (1) is a nonlinear system of delay differential equations (DDEs). For the model analysis we use the software package DDE-BIFTOOL [15, 16].

DDE-BIFTOOL is a Matlab package for bifurcation analysis of systems of DDEs with several discrete delays. The package can be used to compute and analyse the stability of steady state and periodic solutions of a given system as well as to study the dependence of these solutions on system parameters via continuation. The numerical methods implemented in this package are described in [15, 18, 19]. Here we sketch the background on these methods which is necessary to interpret our results and we illustrate the use of the package in the current research. The results obtained in this section are further analysed in Section 5 where the model predictions are studied in detail.

4.1 Steady state solutions

Introduce the notation $S := [V, E_p, E_e, W]^T$ for a vector of solutions of equation (1) and $F := F(S(t), S(t - \tau), S(t - \tau_A), p)$ for a vector defined by the right hand sides of (1) with

p the vector of parameters. A steady state solution, S^* , of (1) is a solution of the nonlinear algebraic system, $F(S^*, S^*, S^*, p) = 0$, or

$$\begin{cases} \beta V(1 - \frac{V}{V_{mvc}}) - \gamma_{VE} E_e V = 0, \\ \alpha_{E_p}(E_p^0 - E_p) + \frac{b_p}{(1+W/\theta_p)^2} V E_p - \alpha_{AP} V^2 E_p = 0, \\ \frac{b_d}{(1+W/\theta_E)^2} V E_p - b_{EV} V E_e - \alpha_{AE} V^2 E_e - \alpha_{E_e} E_e = 0, \\ b_W V - \alpha_W W = 0. \end{cases} \quad (2)$$

This system is solved by a Newton iteration starting from an initial guess for S^* .

The linearization of (1) around a solution trajectory $S^*(t)$ is the variational equation,

$$\frac{d}{dt}y(t) = A_0(t)y(t) + A_1(t)y(t - \tau) + A_2(t)y(t - \tau_A), \quad (3)$$

where A_i equals the derivative of F with respect to its $(i + 1)$ -th argument evaluated at $S^*(t)$.

For a steady state solution, $S^*(t) \equiv S^*$, the matrices $A_i(t)$ are constant, $A_i(t) \equiv A_i$, and the variational equation (3) leads to a characteristic equation,

$$\det(\lambda I - A_0 - A_1 e^{-\lambda\tau} - A_2 e^{-\lambda\tau_A}) = 0, \quad (4)$$

with I the identity matrix and $\lambda \in \mathbb{C}$. The real parts of the characteristic roots λ determine the stability of the steady state solution S^* : the solution is stable if $\Re(\lambda) < 0$ for all λ and it is unstable if a λ exists with $\Re(\lambda) > 0$. In general, (4) has an infinite number of roots. However, it is known that $\Re(\lambda_j) \rightarrow -\infty$ as $j \rightarrow \infty$ and that the number of roots in any right half plane $\Re(\lambda) > \eta$, $\eta \in \mathbb{R}$, is finite. Hence, the stability is always determined by a finite number of roots. The rightmost (stability determining) characteristic roots are approximated using a linear multi-step method applied to variational equation (3), see [15, 16, 19] for details. A steplength heuristic is implemented to ensure accurate approximations of the roots with real part greater than a given constant. The approximations thus obtained are corrected using a Newton iteration on the characteristic equation.

Dependence of the steady state solution S^* on a physical parameter (a component of p) can be studied by computing a branch of steady state solutions as a function of the parameter using a continuation procedure [15]. The stability of the steady state can change during continuation whenever characteristic roots cross the imaginary axis. Generically a *fold* bifurcation (or *turning point*) occurs when a real characteristic root passes through zero and a *Hopf* bifurcation occurs when a pair of complex conjugate characteristic roots crosses the imaginary axis. Once a Hopf point is detected it can be followed in a two parameter space using an appropriate determining system [15]. In this way, for instance, one can compute the stability region of the steady state solution in the two parameter space (if no other bifurcations occur in this region).

We briefly outline a representative example of the stability analysis methodology for model (1) by analysing the effect of the viral exponential growth rate β . To start the analysis, we fix $\alpha_{E_e} = 0.3$, $\alpha_{E_p} = 0.01$ consistent with CTL memory turnover characteristics of Table 2 and all other parameters as in Table 1 (values of b_p , b_d , γ_{VE} and τ of Table 1 are in the admissible ranges of Table 2). We examine the dependence of the corresponding steady state on the parameter β using $\beta \in [0, 3.35]$ as a continuation parameter. The corresponding branch of steady state solutions (depicted in Fig. 2) was computed using the continuation procedure and its stability

was assessed by computing the rightmost characteristic roots with $\Re(\lambda) > -0.3$. One can see that for $\beta = 3.35$ the steady state is unstable because $\Re(\lambda_{1,2}) \approx 0.119 > 0$. At $\beta \approx 1.675$ the steady state is stabilised through a Hopf bifurcation and it remains stable until $\beta = 0$. As $\beta \rightarrow 0$, a real characteristic root approaches zero and the computed solution approaches the steady state solution $S^* = [0, 265, 0, 0]^T$ which exists for all values of the system parameters. Note that the value of V is low, $V \approx 129$ pfu/ml, and almost constant along the computed branch, except near $\beta \approx 0$ where it rapidly decreases to $V = 0$ (see Fig. 2 (left)).

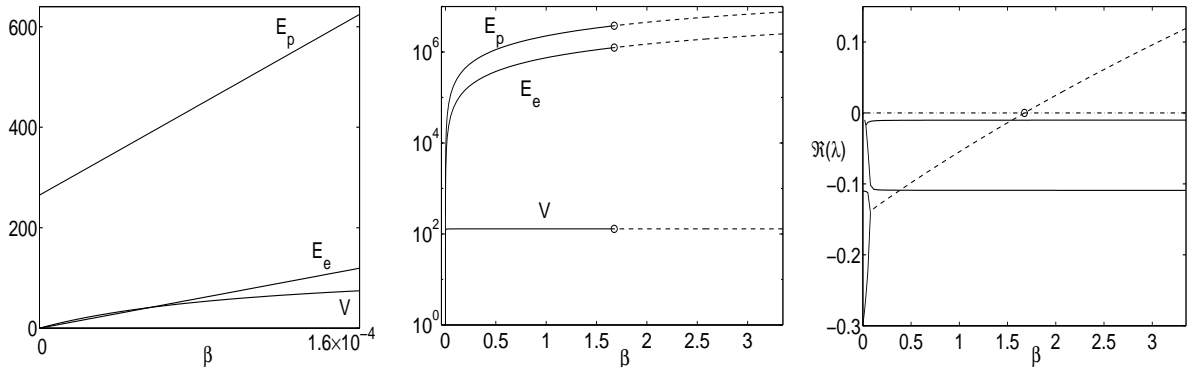


Figure 2: Left, middle: Solutions V (pfu/ml), E_p (cell/ml) and E_e (cell/ml) along a branch of steady state solutions of (1) versus parameter β for $\alpha_{E_c} = 0.3$, $\alpha_{E_p} = 0.01$. Left figure is a blow up of the middle figure. Stable and unstable parts of the branch are denoted by solid, respectively dashed lines. Right: Real part of the rightmost roots (real (—) and complex (---) roots) of the characteristic equation along the same branch. Hopf bifurcation (\circ) at $\beta \approx 1.675$.

4.2 Periodic solutions

A periodic solution $S^*(t)$ is a solution which repeats itself after a finite period T , i.e. $S^*(t+T) = S^*(t)$ for all $t > 0$. A discrete approximation to a periodic solution on a mesh in $[0, T]$ and its period are computed as solutions of corresponding periodic boundary value problem using piecewise polynomial collocation [18, 17].

Stability of a periodic solution is determined by the spectrum of the linear so-called monodromy operator which integrates the variational equation (3) around $S^*(t)$ from time $t = 0$ over the period T . Any nonzero eigenvalue μ of this operator is called a characteristic (Floquet) multiplier. Furthermore, $\mu = 1$ is always an eigenvalue and it is referred to as the trivial Floquet multiplier. The periodic solution is stable if all multipliers (except the trivial one) have modulus larger than 1 and it is unstable if there exists a multiplier with modulus larger than 1. A discrete approximation of the monodromy operator, a matrix M , is obtained using the collocation equations. The eigenvalues of M form approximations to the Floquet multipliers.

A branch of periodic solutions can be traced as a function of a system parameter using a continuation procedure [15]. The branch can be started from a Hopf point or from an initial guess (e.g. resulting from time integration). Bifurcations of periodic solutions occur when Floquet multipliers move into or out of the unit circle. Generically this is a *turning* point when a real multiplier crosses through 1, a *period doubling* point when a real multiplier crosses through -1

and a *torus* bifurcation when a complex pair of multipliers crosses the unit circle.

To illustrate the application of DDE-BIFTOOL to periodic solutions analysis, we computed a branch of stable periodic solutions of (1) as a function of the virus growth rate β , see Fig. 3. This branch emanates from the Hopf point shown in Fig. 2. In Fig. 3, variation of solutions along this branch is characterised by their maximal and minimal values over the period for each computed point on the branch, i.e. $V_{\max}(\beta) = \max_{t \in [0, T]} V(\beta, t)$, $V_{\min}(\beta) = \min_{t \in [0, T]} V(\beta, t)$, etc. The period of the solutions along the branch grows from $T \approx 9.3$ days (Hopf point) to $T \approx 29.6$ days ($\beta = 3.35$).

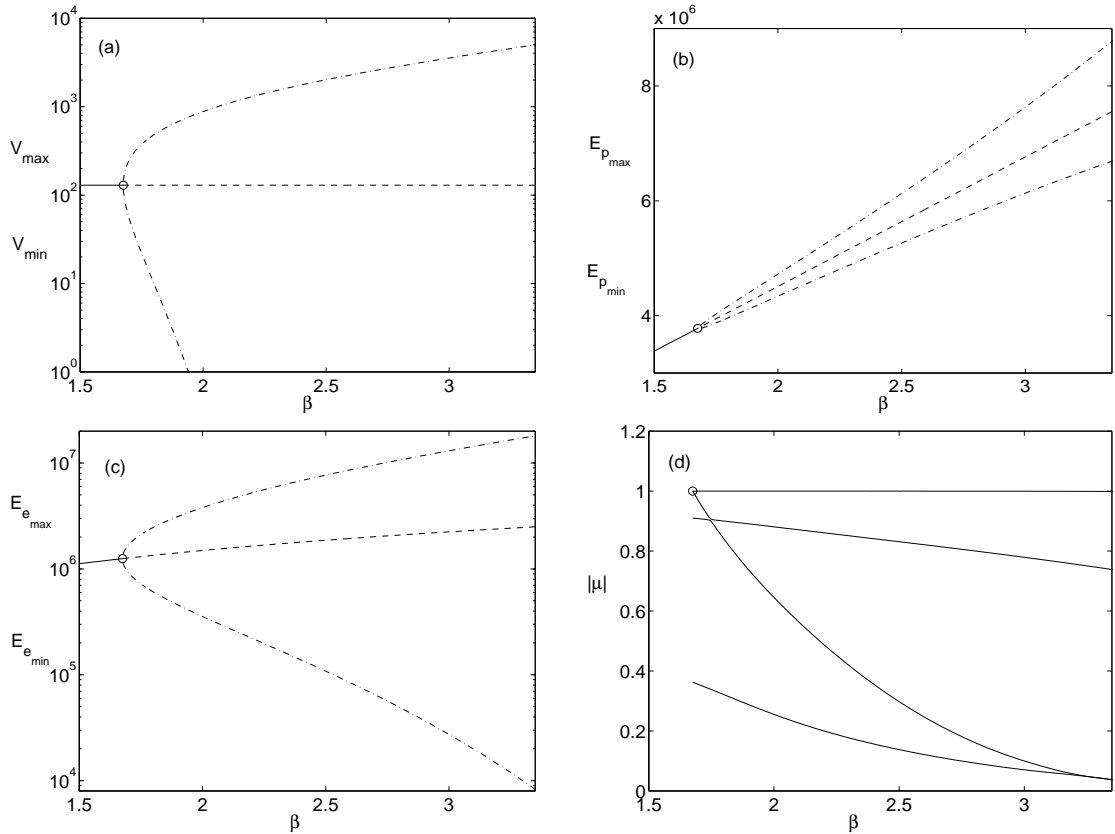


Figure 3: Maximal and minimal values of V (pfu/ml) (a), E_p (cell/ml) (b), E_e (cell/ml) (c) and moduli of the computed dominant Floquet multipliers (d) along a branch of periodic solutions of (1) emanating from the Hopf point (\circ) versus parameter β for $\alpha_{E_e} = 0.3$, $\alpha_{E_p} = 0.01$. (a)-(c): branches of stable (—) and unstable (---) steady state solutions as shown in Fig. 2 and branch of stable periodic solutions (-·-). $0 < V_{\min} < 1$ pfu/ml for $\beta > 1.94$.

4.3 Accuracy of computations

Steady state solutions, periodic solutions, characteristic roots and Floquet multipliers are computed with a certain accuracy determined by the corresponding parameters of the methods implemented in DDE-BIFTOOL. One can use default values for these parameters or specify own desirable values.

A rather small number of mesh points over the period of a periodic solution is often enough to compute a reasonable approximation to the solution, but can be insufficient to obtain good accuracy for the Floquet multipliers. These should be computed with enough accuracy to detect bifurcation points correctly. The accuracy of the trivial multiplier can be used as a first simple check on the accuracy of computations. When necessary the accuracy of the computed multipliers can be improved by refining the discretization of the periodic solution over its period (i.e. by increasing the mesh size).

In our computations, we chose the mesh size such that the trivial multiplier has at least 4-5 digits of accuracy. Some typical accuracy results for two periodic solutions computed on different mesh sizes are given in Table 3. These solutions belong to the branch of periodic solutions shown further (Section 5.3, Fig. 10). Note that solution 2 is close to a turning point of the branch. In the collocation method, we used Gauss-Legendre collocation points, polynomials of degree 3 and L subintervals over a period of the computed periodic solution, i.e. the periodic solution is approximated on a mesh of size $(3L + 1)$. Note that a large value of L is necessary to achieve good accuracy for the Floquet multipliers especially if the computed solution is close to a bifurcation point.

L	solution 1 ($\alpha_{E_p} = 0.1$)			solution 2 ($\alpha_{E_p} = 0.1296$)		
	$ \mu_1 - 1 $	μ_2	T	$ \mu_1 - 1 $	μ_2	T
10	8.33e-03	0.6026222	16.5127474	1.01e+00	0.358939	29.0341684
20	5.97e-05	0.6075486	16.5139693	1.01e-02	0.945482	29.5108723
40	6.75e-06	0.6075174	16.5138970	1.79e-03	0.956941	29.5134526
80	8.03e-08	0.6075131	16.5138997	1.97e-05	0.955260	29.5140578
160	7.93e-09	0.6075132	16.5138995	1.38e-06	0.955243	29.5140750

Table 3: The accuracy of the computed trivial multiplier, the second computed multiplier and the period for two points on the branch of periodic solutions of (1) shown in Fig. 10.

Logarithmic scaling of the state variables of model (1) was used in all our computations, i.e. we rewrote the equation with respect to new variables, $\tilde{V} = \log(V)$, $\tilde{E}_p = \log(E_p)$, $\tilde{E}_e = \log(E_e)$, $\tilde{W} = \log(W)$. This scaling is commonly used in numerical analysis of models for cell population dynamics to avoid computational difficulties caused by combinations of very large and small numbers. Note that the original variables of (1) are shown in all figures.

5 Low level viral persistence

In this section we study in detail the model predictions for basic characteristics of the coexistence of a low level viral population and memory CTL subsets using numerical bifurcation analysis of model (1) as outlined in Section 4.

We start with the stability analysis of steady state solutions, i.e. we determine regions for the virus and host parameters (Table 2) where a steady state solution of model (1), representing the coexistence of virus and memory CTL in equilibrium, is stable. Then we study the influence of virus and CTL parameters on the steady state densities of viral and CTL populations. We

end by analysing oscillatory patterns in virus and CTL memory persistence.

Note that changes of the model parameters compared to the values given in Table 1 are indicated in the figure captions. Units of all parameters are given in Table 2. Units of the population densities are pfu/ml for viruses (V) and cell/ml for precursor (E_p) and effector (E_e) CTL subsets.

5.1 Stability of steady states representing virus-CTL memory coexistence

The relevant parameters of virus and CTL memory persistence are those characterising virus replication and precursor-, effector CTL life-spans: β , α_{E_p} and α_{E_e} . We choose the Hopf bifurcation point indicated in Fig. 2, as a starting point to continue a branch of Hopf bifurcation points in the (β, α_{E_p}) -plane, see Fig. 4 (left). The corresponding Hopf curve bounds the stability region of the steady state corresponding to virus population-CTL memory coexistence because no other bifurcations were found in this region. Using a sequence of similar continuations, we computed branches of Hopf points in the (β, α_{E_p}) -plane for different values of α_{E_e} , see Fig. 4 (right). Whenever $\alpha_{E_p} < 0.9\alpha_{E_e}$, it can be shown that the numerically established stability regions in the three parameter space can be approximated by the formula,

$$\beta < 1.7 - 1.8\alpha_{E_p}/\alpha_{E_e}, \quad (5)$$

describing the nature of the coupling between the parameters necessary to ensure a stable steady state with viral persistence and CTL memory. It indicates an opposite effect of parameters α_{E_p} and α_{E_e} on the value of β .

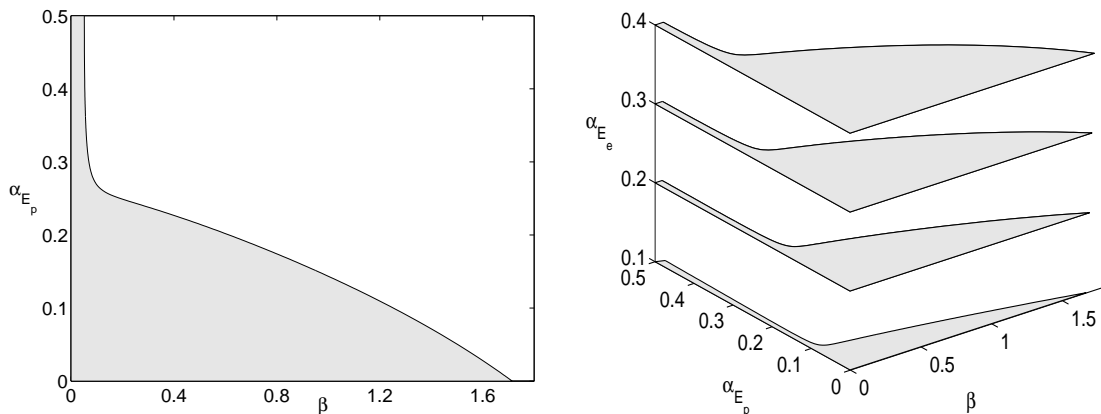


Figure 4: Stability regions (depicted in grey) of the steady state solution of (1) in the (β, α_{E_p}) -plane (left) and in the $(\beta, \alpha_{E_p}, \alpha_{E_e})$ -space (right). Left: $\alpha_{E_e} = 0.3$. Right: Stability regions are visualised for $\alpha_{E_e} = 0.1, 0.2, 0.3, 0.4$. Solid lines correspond to curves of Hopf bifurcations.

Some information about the numerical values of virus and CTL population densities for the steady states in the stability region shown in Fig. 4 (left) is given in Fig. 5. Figure 5 (left) presents the regions in the (β, α_{E_p}) -plane where virus persists below the detection limit ($V < 10^3$

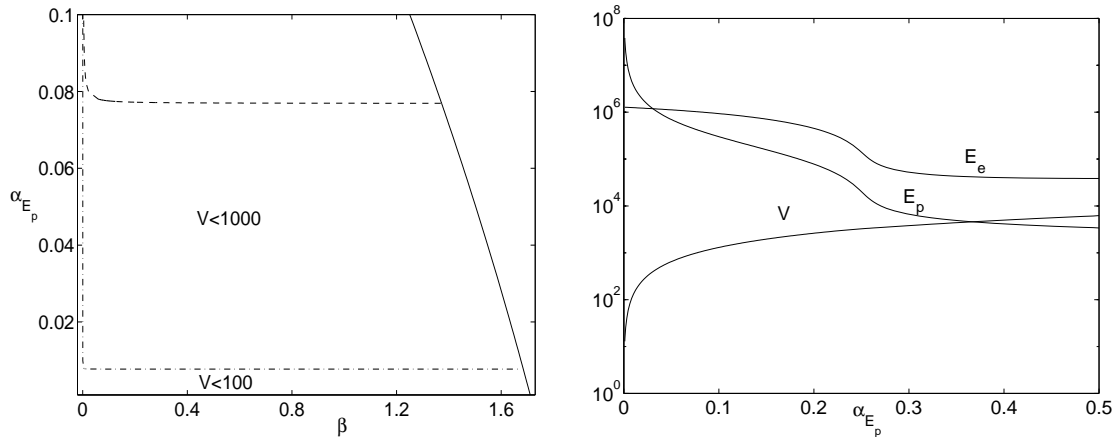


Figure 5: Left: Regions in the (β, α_{E_p}) -plane corresponding to solutions with $V < 1000$ pfu/ml and $V < 100$ pfu/ml. The solid line denotes a Hopf bifurcation curve. Right: Steady state solutions V (pfu/ml), E_p (cell/ml) and E_e (cell/ml) along the Hopf curve shown in Fig. 4 (left).

pfu/ml) and below 10^2 pfu/ml. One can see that the value of V almost does not depend on β unless β gets close to 0 (see also Fig. 2) and virus can persist at a very low level if the death rate of CTLp (α_{E_p}) is small enough. In Fig. 5 (right) we present steady state values of V , E_p and E_e along the branch of Hopf points as a function of parameter α_{E_p} . Notice that each value of α_{E_p} corresponds to a certain value of β on the branch of Hopf points. The maximum value of persisting virus population V along the Hopf curve, $V \approx 6250$ pfu/ml, is reached at point $\alpha_{E_p} = 0.5$, $\beta \approx 0.052$. Hence $V < 6250$ pfu/ml in the stability region shown in Fig. 4 (left).

As it is shown further (Fig. 8 (c)), changes of α_{E_e} in the interval $[0.1, 0.4]$ have little impact on the equilibrium values of the virus population V . This implies that the features shown in Fig. 5 remain true for $\alpha_{E_e} \in [0.1, 0.4]$.

Influence of τ . An increase of the delay τ has a strong effect and decreases the size of the stability regions, see Fig. 6. For other values of α_{E_e} than the one used in Fig. 6, the changes are qualitatively similar.

Influence of b_p . Interestingly, a decrease rather than an increase in the CTL stimulation rate b_p has a stronger influence on the size of the stability region, see Fig. 7 (left). About 10-fold decrease in b_p requires $\alpha_{E_p} < 0.01$ rather than 0.08 as before to ensure viral persistence with $V < 10^3$ pfu/ml, see Fig. 7 (right).

Similar analysis shows that variations of the parameters b_d and γ_{VE} within their ranges (cf. Table 2) do not change the stability regions significantly.

So, the model predicts that low level viral persistence as an equilibrium state is possible under the condition that the replication rate of virus, β , in the immune mice is smaller than the one during acute infection. The maximal value of the replication rate of (low level) persisting virus depends on the CTL turnover parameters in the way specified by (5) and shown by the above figures. In particular, the slower turnover of CTL memory is, the smaller the maximal replication rate of the persisting virus must be.

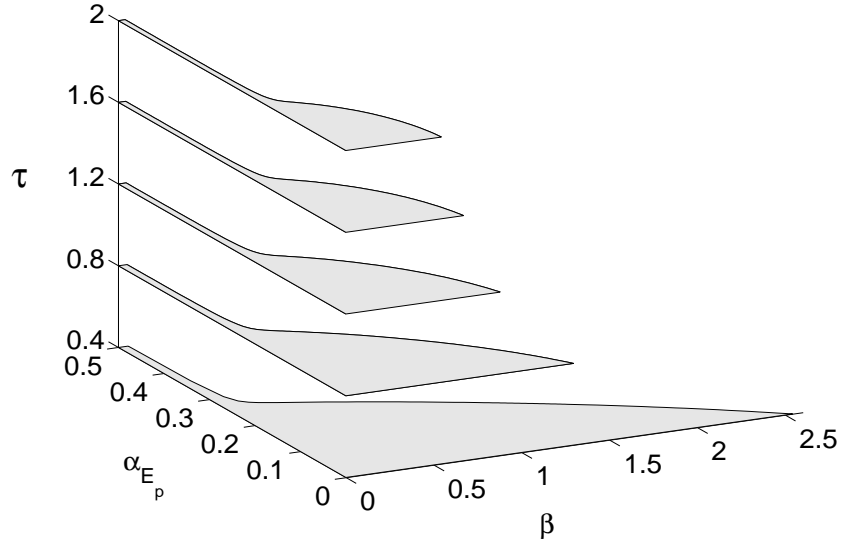


Figure 6: Stability regions (depicted in grey) of the steady state solution of (1) in the $(\beta, \alpha_{E_p}, \tau)$ -space for $\tau = 0.4, 0.8, 1.2, 1.6, 2$. Solid lines correspond to curves of Hopf bifurcations. $\alpha_{E_e} = 0.3$.

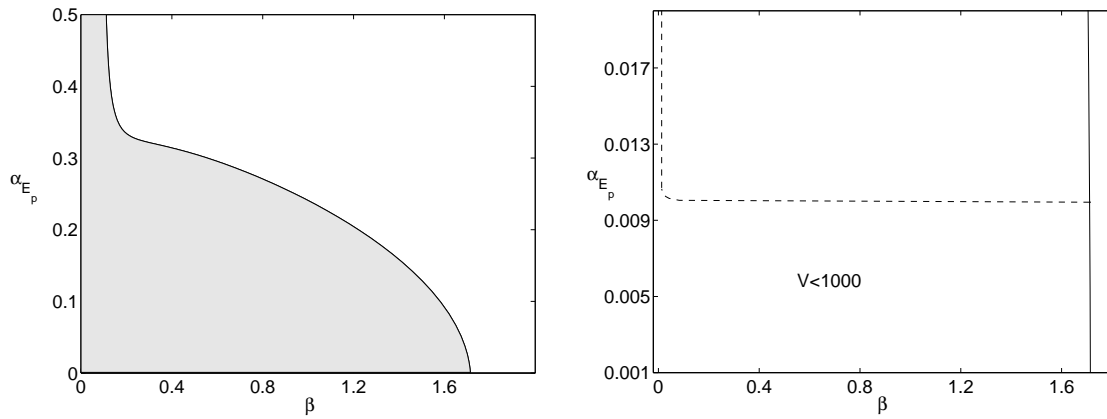


Figure 7: In the (β, α_{E_p}) -plane, stability region (depicted in grey) of the steady state solution of (1) (left) and region corresponding to solutions with $V < 1000$ pfu/ml (right) for $b_p = 10^{-5}$. $V < 100$ pfu/ml for $\alpha_{E_p} < 0.001$. The solid line denotes a Hopf bifurcation curve. $\alpha_{E_e} = 0.3$.

5.2 Effect of virus and CTL parameters on the level of persisting virus and composition of CTL memory

We proceed with the analysis of the influence of virus and CTL parameters β , α_{E_p} , α_{E_e} , b_p , b_d and γ_{VE} on the coexisting population densities of the virus, precursor CTLs and effector CTLs. The behaviour of steady state solutions of (1) V , E_p and E_e is examined by varying the parameters within their ranges specified in Table 2. As a starting point, we use the stable steady state solution, $V \approx 129$ pfu/ml, $E_p \approx 2.3 \cdot 10^6$ cell/ml, $E_e \approx 7.5 \cdot 10^5$ cell/ml, $W \approx 1.2 \cdot 10^3$ pfu/ml, which corresponds to parameters $\beta = 1$, $\alpha_{E_p} = 0.01$, $\alpha_{E_e} = 0.3$ and other parameter values as in Table 1 (see Fig. 2). Then, branches of steady state solutions are computed as functions of the above parameters.

Influence of β . The level of viral persistence is not affected by changes of the virus replication rate unless the latter gets very small, see Fig. 2. However, a faster replicating virus needs more precursor and effector CTL for stable coexistence.

Influence of α_{E_p} . The increase in the life span of precursor CTL leads to an increase of steady state number of CTLp and to a decrease in the level of viral persistence, see Fig. 8 (a). Note that at $\alpha_{E_p} \approx 0.143$ the steady state solution undergoes a Hopf bifurcation (see Fig. 4 (left)) and we continued the branch of steady states for $\alpha_{E_p} \in [0.001, 0.143]$.

Influence of b_p . The rate constant of CTL stimulation to division has a strong impact on the level of persisting virus, see Fig. 8 (b). More sensitive precursor CTL population needs less virus for the same extent of stimulation, so that a 10-fold increase of b_p (from $b_p = 10^{-4}$ to $b_p = 10^{-3}$) leads to 10-fold decrease of V .

Influence of α_{E_e} . When the life span of effector CTLs increases from 2.5 to 10 days (corresponding to $\alpha_{E_e} \in [0.1, 0.4]$), a smaller number of precursor CTL is enough to maintain the same amount of the virus in a stable equilibrium state, see Fig. 8 (c).

Influence of b_d . When the rate constant of CTL differentiation increases, a smaller number of precursor CTL is enough to maintain the same amount of virus under control, see Fig. 8 (d). For instance, 10-fold increase of b_d (from $b_d = 10^{-3}$ to $b_d = 10^{-2}$) leads to (almost) 10-fold decrease of E_p .

Influence of γ_{VE} . Changes in the rate constant of virus clearance almost do not affect the level of persisting virus, see Fig. 8 (e). However, for smaller values of γ_{VE} larger numbers of precursor and effector CTLs are necessary to maintain persistence of the virus population at the same level.

Note that under the condition $V \ll V_{mvc}$, which is fulfilled in the case of low level viral persistence, an approximate steady state density of virus, precursor CTL and effector CTL populations can be obtained from model (1) as

$$V \approx \frac{\beta \alpha_{E_e} \alpha_{E_p}}{\gamma_{VE} \alpha_{E_p} b_d E_p^0 + \beta \alpha_{E_e} b_p}, \quad E_p \approx E_p^0 + \frac{\beta \alpha_{E_e} b_p}{\gamma_{VE} \alpha_{E_p} b_d}, \quad E_e \approx \frac{\beta}{\gamma_{VE}}.$$

These approximations are in agreement with the results presented in Fig. 8 and clearly indicate effect of virus and CTL parameters on the populations level.

The above results (Sections 5.1 and 5.2) are briefly summarised in Table 4. Note that influence of the delay τ appears only in the first row of this table since the position of steady state solutions of delay equations does not depend on the delay value but their stability does.

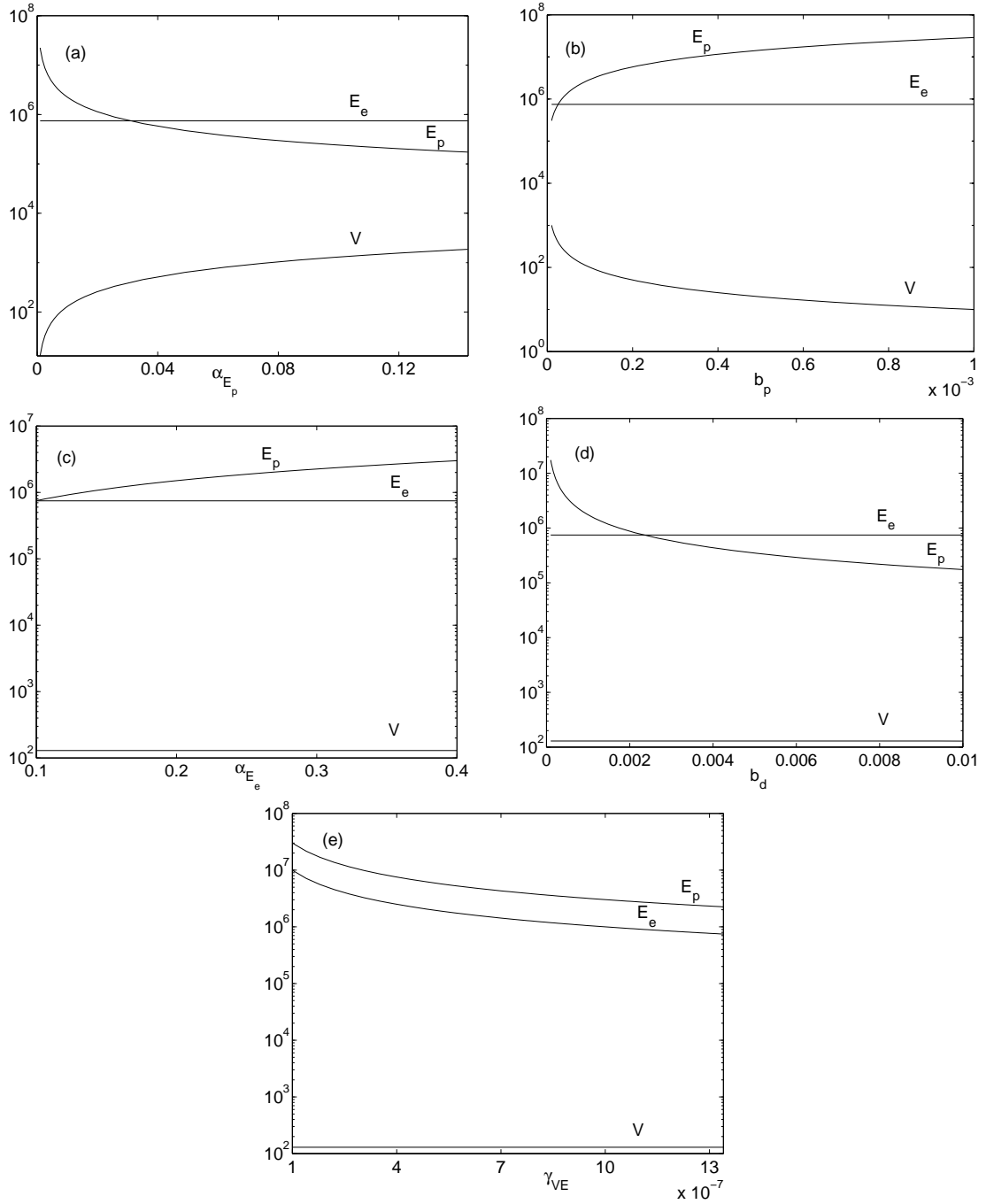


Figure 8: Evolution of V (pfu/ml), E_p (cell/ml) and E_e (cell/ml) along branches of steady state solutions of (1) versus parameters α_{E_p} (a), b_p (b), α_{E_e} (c), b_d (d) and γ_{VE} (e). $\alpha_{E_p} = 0.01$, $\alpha_{E_e} = 0.3$ except for figures (a) and (c), respectively. $\beta = 1$.

	β	α_{E_p}	α_{E_e}	b_p	b_d	τ	γ_{VE}
Probability of the virus and memory CTL coexistence as an equilibrium state	↓	↓	↑	↓	≈	↓	≈
Level of virus persistence	≈	↑	≈	↓	≈		≈
Size of precursor CTL memory	↑	↓	↑	↑	↓		↓
Size of effector CTL memory	↑	≈	≈	≈	≈		↓

Table 4: Effect of *increasing* the values of virus and CTL parameters (β , α_{E_p} , α_{E_e} , b_p , b_d , τ and γ_{VE}) on the characteristics of low level viral persistence (below the detection limit of conventional assays, i.e. 100 pfu/spleen) and CTL memory populations. The case of insignificant influence of a parameter is denoted by \approx .

5.3 Oscillatory patterns of viral persistence

In the neighbourhood of a Hopf bifurcation point, solutions which belong to a branch of periodic solutions emanating from this point oscillate around the steady state value corresponding to the Hopf point. Hence Hopf points with low values of V can be sources of periodic solutions with oscillatory low level viral persistence. We use the Hopf point shown in Fig. 2 as our “basic Hopf point” and study the existence of oscillatory patterns in viral persistence by computing branches of periodic solutions emanating from this point as a function of the parameters listed in Table 2. Note that we depict periodic solutions on the time interval $[0, 1]$, i.e. after time is scaled by the factor T^{-1} with T the period of the solution.

Influence of β . As β grows from its Hopf point value ($\beta \approx 1.675$), the amplitude of oscillations of $V(t)$ grows rapidly, see Fig. 3. The sensitivity of the dynamics to changes of β is also well characterised by the fact that a subtle change in β (from 1.675 to 2.06) leads to “pulse” oscillations in virus population size, see Fig. 9 where solutions are shown for three values of β : close to the Hopf point (a), when $V_{\max} \approx 10^3$ pfu/ml (b) and when $V_{\max} \approx 2 \cdot 10^3$ pfu/ml (c).

Influence of α_{E_p} . When continuing a branch of periodic solutions with respect to α_{E_p} , the branch turns twice changing its stability, see Fig. 10. The changes in stability are illustrated in Fig. 10 (e), where the moduli of the computed dominant Floquet multipliers along this branch are depicted versus an approximation of the arclength of the branch. For $\alpha_{E_p} \in [0.078, 0.130]$, two stable periodic solutions exist indicating a *hysteresis* phenomenon. The latter implies that a “jump” to another stable periodic solution (caused by a turning point of the branch) happens at $\alpha_{E_p} \approx 0.078$ or at $\alpha_{E_p} \approx 0.130$ depending on whether the periodic solution being traced belongs to the lower or to the upper stable part of the branch. Note that both the amplitude and the period of oscillations along the upper stable part of this branch are very large and hence such oscillatory solutions are not biologically realistic. The amplitude of oscillations of $V(t)$ grows rapidly as α_{E_p} increases (see Fig. 10 (b)) and the oscillations approach a “pulse form”, see Fig. 11, where periodic solutions are shown for the values of α_{E_p} such that the peaks of $V(t)$ along the period are about the same as in Fig. 9.

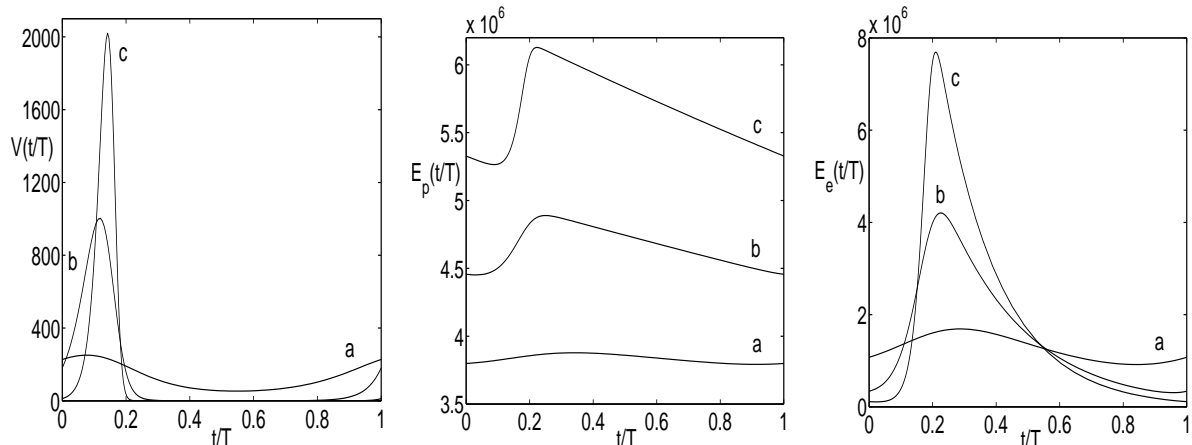


Figure 9: Sensitivity of periodic solutions to changes in virus growth rate, β . Solutions V (pfu/ml), E_p and E_e (cell/ml) corresponding to three points on the branch of periodic solutions shown in Fig. 3: $\beta = 1.7$ (a), $\beta = 2.06$ (b), $\beta = 2.5$ (c). Values of the period T (days): $T \approx 9.5$ (a), $T \approx 13.2$ (b), $T \approx 18.2$ (c).

To study existence of periodic solutions in relation to viral growth and precursor CTL death rate constants, i.e. in the (β, α_{E_p}) -plane, we computed branches of periodic solutions versus α_{E_p} for some values of β in the interval $[0.1, 3.35]$. In this way we found turning points of periodic solutions in the (β, α_{E_p}) -plane. We summarised the results in Fig. 12 where the curves of these turning points bound regions with different numbers of (stable and unstable) periodic solutions. Note that left parts of the curves of turning points end at Hopf bifurcation points of steady state solutions. The dynamic complexity of the system is well characterised by the fact that in region 3 steady state solutions coexist with periodic solutions and in region 2 two stable periodic solutions coexist. However, the region of our interest, where periodic oscillations are such that $V_{\max} < 10^3$ pfu/ml, is quite small. Much smaller is the region with V varying between 10 to 10^3 pfu/ml (or equivalently between 1 to 100 pfu/spleen), see Fig. 12 (right). In this region the period of oscillations varies from 10 to 20 days.

Influence of b_p . Larger values of b_p increase the region in the (β, α_{E_p}) -plane where oscillatory solutions with $V_{\max} < 10^3$ pfu/ml exist, see region A in Fig. 13. However, due to a high sensitivity of the amplitude of oscillations to changes in values of β and α_{E_p} the region where $V_{\min} > 10$ pfu/ml (B) remains quite small. Although two stable periodic solutions coexist in a part of region A, one of them is not biologically realistic because of very large values of the amplitude and the period of oscillations. Note that the upper left part of region A is bounded by the curve of turning points (which ends at a Hopf point), i.e. for the corresponding values of β and α_{E_p} periodic solutions lose stability before V_{\max} reaches 10^3 pfu/ml.

The effect of the other parameters can be briefly summarised as follows.

Influence of α_{E_e} . As α_{E_e} decreases from 0.3 (Hopf point) to 0.1, the period of oscillations increases to 22 days and V_{\max} increases to 950 pfu/ml. For $\alpha_{E_e} = 0.1$ Hopf bifurcation occurs at $\beta \approx 1.54$, which implies that for $\alpha_{E_e} = 0.1$ the value of V_{\max} grows from 129 to 950 pfu/ml as β changes from 1.54 to 1.675. Hence for $\alpha_{E_e} \in [0.1, 0.4]$ the size of the region in (β, α_{E_p}) -plane where $V_{\max} < 10^3$ pfu/ml is also quite small and the location of this region with respect to the

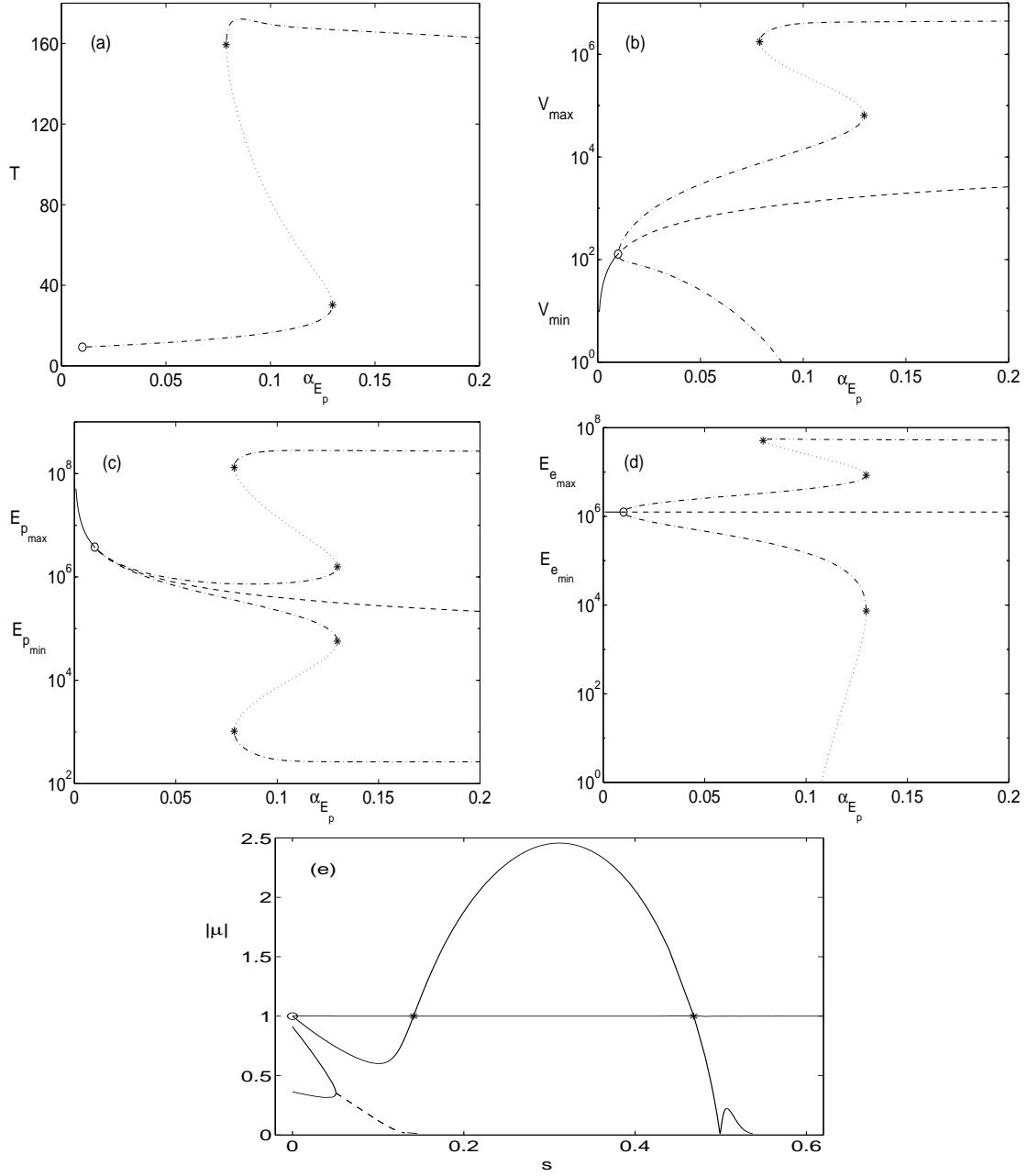


Figure 10: Period T (days) (a), evolution of maximal and minimal values of V (pfu/ml) (b), E_p (cell/ml) (c) and E_e (cell/ml) (d) along a branch of periodic solutions of (1) emanating from the Hopf point (\circ) versus parameter α_{E_p} for $\alpha_{E_e} = 0.3$, $\beta \approx 1.675$. Branches of stable (—) and unstable (---) steady state solutions and branches of stable (—) and unstable (·) periodic solutions. (e): Moduli of the computed dominant Floquet multipliers (real (—) and complex (---)) versus the arclength s of the same branch. (*) - turning points ($\alpha_{E_p} \approx 0.130$, $\alpha_{E_p} \approx 0.078$).

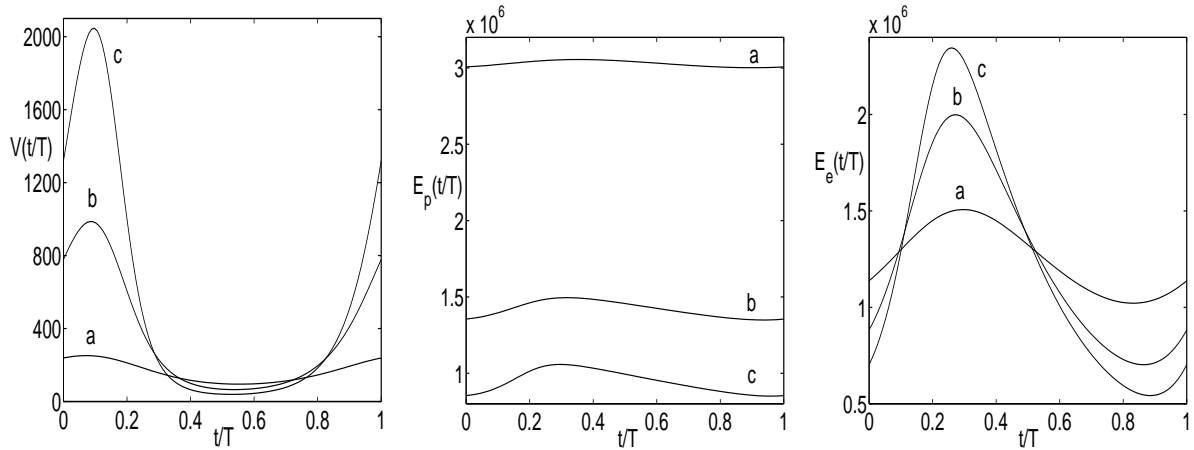


Figure 11: Sensitivity of periodic solutions to changes in CTLp death rate, α_{E_p} . Solutions V (pfu/ml), E_p and E_e (cell/ml) corresponding to three points on the branch of periodic solutions shown in Fig. 10: $\alpha_{E_p} = 0.0125$ (a), $\alpha_{E_p} = 0.027$ (b), $\alpha_{E_p} = 0.041$ (c). Values of the period T (days): $T \approx 9.4$ (a), $T \approx 10.2$ (b), $T \approx 11.0$ (c).

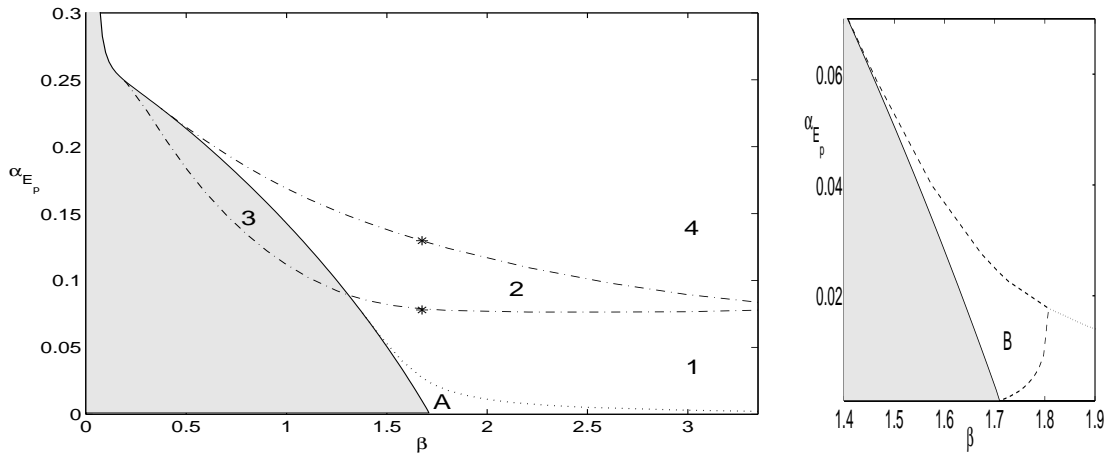


Figure 12: Left: Stability region (depicted in grey) of the steady state solution and Hopf curve (solid line) as in Fig. 4 (left). Two curves of turning points (---) of periodic solutions. (*) - two turning points depicted in Fig. 10. Regions of existence of periodic solutions: 1 stable solution (1,4), 2 stable and 1 unstable solution (2), 1 stable and 1 unstable solutions (3). The dotted line bounds a region (A) of existence of periodic solutions with $V_{\max} < 10^3$ pfu/ml. Right: A blow up of the left figure. The dashed line bounds a region (B) where $V_{\min} > 10$ pfu/ml, i.e. the region with V varying between 1 to 100 pfu/spleen. $\alpha_{E_e} = 0.3$.

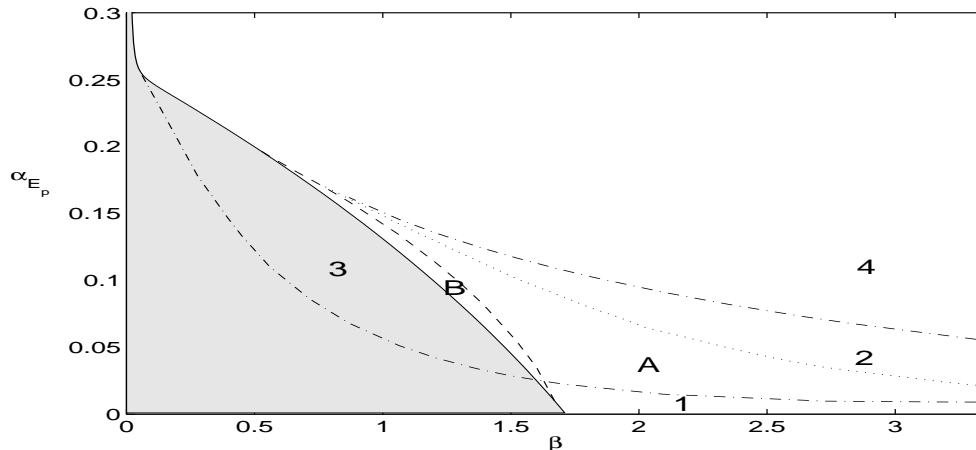


Figure 13: Stability regions of steady state and periodic solutions for $b_p = 10^{-3}$. All notations are analogous to Fig. 12. $\alpha_{E_c} = 0.3$.

corresponding Hopf curve is similar to the one shown in Fig. 12.

Influence of τ . As τ increases from 0.6 (Hopf point), the amplitude of oscillations grows rapidly and V_{\max} reaches 10^3 pfu/ml at $\tau \approx 0.8$. At this point the period of oscillations is about 15 days. For $\tau = 0.8$ Hopf bifurcation occurs at $\beta \approx 1.3$, which implies that for $\tau = 0.8$ the value of V_{\max} grows from 129 to 10^3 pfu/ml as β changes from 1.3 to 1.675. Hence for $\tau = 0.8$ the size of the region in (β, α_{E_p}) -plane where $V_{\max} < 10^3$ pfu/ml is also quite small and the location of this region with respect to the corresponding Hopf curve (see Fig. 6) is similar to the one shown in Fig. 12.

Variations of parameters b_d and γ_{VE} within the admissible ranges of Table 2 have much lesser impact on the amplitude of oscillations compared to variations of β , α_{E_p} and τ and do not change it significantly.

Overall, we found that the periodic solutions with V varying between 10 to 10^3 pfu/ml exist in quite narrow intervals of β and α_{E_p} values and the amplitude of oscillations grows rapidly as parameters β , α_{E_p} and τ increase. So the model predicts that oscillatory patterns in low level viral persistence (with virus population varying between 1 to 100 pfu/spleen) are possible for quite “special” combinations of the rates of virus growth and precursor CTLs death because of a high sensitivity of the amplitude of oscillations to changes in the above parameters.

6 Discussion

Virus persistence is an intriguing area of current biological interest. The murine LCMV system provides one of the most extensively documented experimental infection to examine how simple viruses can escape complete elimination from an immunocompetent host [56]. It has recently been shown that a *low level* (i.e. below the limit of detection by conventional assays about 10^2 pfu per spleen or equivalently 10^3 pfu/ml of spleen) long-term persistence of replication competent LCMV in the immune mice is possible [9, 24, 38, 54]. A range of mechanisms, both molecular and immunologic, might be responsible for low level viral persistence in the face of CTL

memory [3, 24, 40, 43, 50, 51]. In this paper we analyse in quantitative terms the *kinetic basis* of coexistence of a small virus population with precursor and effector CTLs during the memory persistence phase after primary infection, i.e. the combination of growth and death rates of virus and CTL populations for which a stable coexistence is possible. The study is based on the numerical bifurcation analysis of a mathematical model which is quantitatively consistent with relevant data on virus and CTL dynamics in the primary LCMV-Docile infection of C57BL/6 mice [7, 14].

Equilibrium state.

Low level viral persistence and memory CTL. The main result of our analysis is that unless LCMV replication rate does not reduce to smaller values, as compared to that during the acute phase of primary infection, low level persistence in the face of CTL memory as an equilibrium state is not possible: the virus will either be cleared or establishes a high viral load chronic infection, both outcomes depending on the initial dose of infection and the relative kinetics of viral growth. The extent of reduction needed depends on the responder status of the host, in particular, the life-span of CTL memory subsets, duration of CTL division cycle, activation thresholds of CTL for proliferation and differentiation. Since the virus remains the same during acute and persistence phase (it should not acquire attenuating mutations) we propose that the reduction in LCMV replication rate resulting in the low level persistence could be either due to changes in the host cells, e.g. mediated by interferons (IFN_α), or an intrinsic features of the virus replicatory cycle [27], which slow down the virus growth. This mechanism seems to be in agreement with virus reappearance after initial elimination below detection levels in $CD4^+$ T cell help deficient mice, since the deficiency primarily impairs the LCMVs-specific IFN_γ production by CTLs and $CD4^+$ T cells.

Our analysis predicts that LCMV can coexist with expanded clone of virus-specific CTL in the memory phase below the limit of its detection if the per day relative increase of the virus population (similar to the notion of basic reproductive number [4]) reduces about 5 fold, i.e. from 29 to 6. In this case the virus maintains the splenic memory CTL population of about $10^6 - 10^8$ cells/ml. In the model, the size of the effector CTL memory population in the case of low level viral persistence is determined by the ratio of virus exponential growth rate to the CTL-mediated virus elimination rate and is, therefore, independent of other CTL response parameters. The virus replication rate appears not to affect the steady state level of the LCMV population except for extremely low values, when the equilibrium size becomes smaller than 1 pfu. Therefore, the maintenance of CTL memory through low level viral persistence implies that a fraction of the memory CTL population is represented by effector CTLs that control the virus population in a balanced way. This means biologically that the phenotype of the CTL memory in case when small virus population persists would include an enhanced capacity to mediate effector function, ensuring a better protection. Therefore, a functional CTL memory implies low level virus persistence and vice versa. A remarkable prediction of the above analysis is that for the biologically realistic range of CTL memory parameters (see Table 2) the level of virus persistence is compatible with 10 to 100 pfu per spleen, i.e. the detection limit of conventional assays. The persistence of virus population at levels essentially larger than 100 pfu for the studied parameter ranges appears to be biologically unrealistic because its dynamics is oscillatory with the bottom number of LCMV less than 1 pfu, which means complete elimination.

Effects of precursor and effector CTL death rates. Parameters characterising the death rates of precursor and effector CTL subsets of the memory population have a major impact on the stability and the steady state densities of the coexisting precursor CTL and LCMV, yet no effect on the absolute number of effector CTLs: a longer life-span of the precursor CTL leads to smaller level of the persisting virus and increases the number of CTLp, whereas the increase in life-span of effector CTL induces a decrease of CTL precursor density, while not affecting the persistence level of virus population. Thus the model predicts that longer life-span of the memory precursor CTLs ensures a more efficient control of persisting virus population keeping it at lower level.

By varying, within their admissible ranges, the parameters of CTL memory characterising the turnover rates of precursor and effector CTLs we identified domains in the parameter space where a small virus population - CTL memory coexistence is possible. The results show that (i) the level of LCMV persistence falls below 100 pfu/spleen in immune mice with memory precursor CTL having a life-span longer than 12 days; (ii) to a large extent, the possibility of the coexistence itself is mostly affected by the virus replication rate, whereas the size of the virus population is determined by the life-span of the precursor CTLs of memory pool (10-fold increase in the life span reduces the level of viral persistence in the spleen from 100 to about 10 pfu); (iii) the shorter the life-span of effector CTL subset in the memory phase the wider the intervals of values of the virus replication rate and life-span of CTLp for which the coexistence is possible, so that it is easier for the virus to set up low level persistence.

Effects of cell division time and rates of virus elimination and CTLp activation and differentiation. Model parameters representing CTL responsiveness and antiviral efficacy, such as CTL precursor activation rate (b_p), differentiation rate into effectors (b_d), cell division time (τ) and elimination rate of virus (γ_{VE}), differ in their effect on virus-CTL memory coexistence. The parameters of clonal growth rate (b_p, τ) have a much stronger impact on the size of the region in the (α_{E_p}, β) -plane where the coexistence is possible. The increase in b_p or decrease of τ values, that would reflect the situation of *better responder* host [37], ensure that coexistence is possible for a broader combination of (α_{E_p}, β) parameters and, in this sense, provides more favourable conditions for the coexistence of a small virus population with CTL memory. Interestingly, while an increase in CTL activation rate leads to coexistence of larger population of CTL memory and lower level of virus load, an increase in the differentiation rate affects only the precursor subset of CTL memory pool by decreasing it. A decrease in the efficacy of CTL-mediated elimination of the virus has an opposite effect on the maintenance level of CTL memory in the situation of low level viral persistence: a 10-fold decrease in the elimination rate constant leads to a similar increase in the memory populations of precursor and effector CTLs, which is necessary to control virus population in a balanced equilibrium.

Oscillatory dynamics.

Numerical analysis of periodic solutions in the model dynamics suggests that virus and CTLs can also coexist in an oscillatory mode. Although periodic oscillations exist for a broad combination of parameter values, the biologically relevant oscillatory patterns of low level virus persistence are possible only within *narrow* intervals of the rates of virus growth and precursor CTL death which depend on values of other parameters, especially on the rate constant of CTL stimulation. This is a consequence of an exponential-type sensitivity of the amplitude of

oscillations to changes in the rates of virus growth and precursor CTL population death. Note that variation in CTL number during the period of oscillations is much more prominent in the effector compartment than in the precursor compartment, which is due to the shorter life span of the former.

The model predicts that for the combinations of the parameters such that viral load oscillates within the window of 1 to 100 pfu/spleen, the period of oscillations ranges from 10 to 20 days. When oscillations have a “pulse form”, the period can be considered as the time interval between viral “bursts”. These numbers are instructive in understanding viral kinetics in those cases when CTL memory response is not sustained for some reasons and imply that the earliest time of virus re-appearance after initial elimination below detection limit would be 20 to 30 days post infection. To give an example, consider experimental data characterising LCMV specific CTL precursor decay in the spleen of CD4 knock-out mice over 120 days after infection [23]. These data suggest the estimate of 12 days for the half-life of CTLp population. Taking into account that the gradual disappearance of memory CTL might be partly compensated by continuing CTL division the actual life-span seems to be even shorter. For such life-span of CTL (≤ 12 days) the model predicts (Fig. 10) the possibility of oscillations with period ranging from 10 to 30 days. Therefore, if virus drops after primary CTL response below detection limit at day 15 (conventional scenario) than it would reappear in the deficient host in between 20 to 45 days. This range is quantitatively consistent with the bi-phasic viral kinetics observed in CD4⁺ T help deficient mice [42, 49].

Limitations of the analysis.

The mathematical model used in this study is a simplification of the real complexity of virus-host interaction. Although CD8⁺ CTLs are the major effector cells for virus clearance in the LCMV model, the relevance of CD4⁺ T helper cells and B-cells in long term control of low level virus persistence and maintenance of CTL memory was clearly shown [23, 42, 49, 50]. Helper T cells appear to be necessary to sustain functional CTL responses and effect virus clearance through IFN γ production, whereas antibodies primary work by lowering virus spread [5]. To some extent, the impact of T help and antibody responses on the coexistence of a low level virus population and CTL memory can be extrapolated from the above studies of the effect of virus growth rate and turnover, differentiation rates of precursor CTL of the memory pool. Consider, for example, the effect of virus-specific antibodies on the low level viral persistence. Antibodies act through neutralising the free virus particles. Assuming that their concentration is constant, A^* , the effect on the kinetics can be represented by introducing an additional first order decay term in the equation for viruses that describes the elimination of viruses by antibodies, $-\gamma_{VA}V(t)A^*$. This term can be combined with the growth term for the virus and the overall effect would therefore be to reduce the replication rate of virus from β to $\beta - \gamma_{VA}A^*$. Thus, using the results on the impact of β on virus-CTL memory coexistence (see Figs. 4-7, 12, 13) it is possible to predict the impact of a given population of virus-specific antibodies on equilibriums and oscillatory modes in virus-CTL memory coexistence.

Human infections: trace HBV persistence.

The results of our analysis could be useful in understanding the basis for trace viral persistence documented in humans, e.g. after acute infection with hepatitis B virus [30]. Like

LCMV, HBV is a non-cytopathic virus controlled by CTL responses. It was recently directly demonstrated that small amounts of HBV (which are below the detection limits of conventional solid-phase or fluid phase hybridization assays) coexist with, and actively maintain HBV-specific CTL response for many years following recovery from acute viral hepatitis [44]. Although the immunological mechanisms of such low level HBV replication in healthy individuals remain unclear, the kinetic parameters ensuring a long-term stable control of a trace amount of replication competent HBV by memory CTL population can be clarified using a similar approach.

7 Conclusions

It is widely accepted that the outcome of many viral infections is containment rather than eradication of infection [29]. Low level pathogen persistence occurs in a variety of human infections including those of major medical importance, e.g. HBV, HCV and HIV. Understanding the kinetic aspects of this fundamental area of biology is essential in defining host immunity and its failure, in the context of these relevant pathogens.

A growing tendency in modern immunology to deal with the dynamic complexity of virus-host interaction in terms of numbers and kinetic rates [11, 58], needs advanced mathematical modelling and numerical analysis tools. In this paper we examined low level viral persistence in the immune host using a mathematical model of antiviral cytotoxic T cell responses in mice infected by LCMV. The model is described by a nonlinear system of delay differential equations. The predictions on the low level viral persistence and CTL memory are obtained using numerical bifurcation analysis of the model with the software package DDE-BIFTOOL. We showed that the numerical tools offer new possibilities in understanding mechanisms of viral persistence and complex dynamics of the virus-immune system interaction.

We identified the *kinetic limits* of the immune system, in terms of the turnover rates for virus and memory CTLs, in its ability to control a replicating non-cytopathic virus at a low level. The numerical values of the parameters ensuring coexistence of a low level LCMV population and greatly expanded CTLs during the memory phase quantitatively illustrate how the immune system makes use of a large number of lymphocytes in order to compensate an initially unfavourable '*numbers game*' or races with the rapidly replicating virus and makes the virus-host interaction more balanced biologically [58, 59].

Acknowledgements

This research has been supported by Research Council K.U.Leuven (project OT 98/16), the programme on Interuniversity Poles of Attraction for Science, Technology and Culture (IUAP P4/02), the Alexander von Humboldt Foundation, Deutsche Forschungsgemeinschaft and the Wellcome Trust. K. Engelborghs is a Postdoctoral Fellow of the Fund for Scientific Research - Flanders (Belgium). The authors are grateful to Prof. Roy M. Anderson (Imperial College School of Medicine) and Prof. Dirk Roose (Katholieke Universiteit Leuven) for scientific advice and support.

References

- [1] R. Ahmed and D. Gray. Immunological memory and protective immunity: understanding their relation. *Science*, 272:54–60, 1996.
- [2] R. Ahmed, B. D. Jamieson, and D. D. Porter. Immune therapy of a persistent and disseminated viral infection. *J. Virol.*, 61:3920–3929, 1987.
- [3] R. Ahmed, L. A. Morrison, and D. M. Knipe. Viral persistence. In N. Nathanson et al., editor, *Viral Pathogenesis*, pages 181–205. Lippincott-Raven Publishers, Philadelphia, 1997.
- [4] R. M. Anderson and R. M. May. *Infectious Diseases of Humans. Dynamics and Control*. Oxford University Press, Oxford, 1991.
- [5] J. R. Baldrige, T. S. McGraw, A. Paoletti, and M. J. Buchmeier. Antibody prevents the establishment of persistent arenavirus infection in synergy with endogenous T cells. *J. Virol.*, 71:755–758, 1997.
- [6] W. Barchet, S. Oehen, P. Klenerman, D. Wodarz, G. Bocharov, A. L. Lloyd, M. A. Nowak, H. Hengartner, R. M. Zinkernagel, and S. Ehl. Direct quantitation of rapid elimination of viral antigen-positive lymphocytes by antiviral CD8⁺ T cells in vivo. *Eur. J. Immunol.*, 30:1356–1363, 2000.
- [7] G. Bocharov. Modelling the dynamics of LCMV infection in mice: conventional and exhausted CTL responses. *J.theor. Biol.*, 192:283–308, 1998.
- [8] G. Bocharov, P. Klenerman, and S. Ehl. Predicting the dynamics of antiviral cytotoxic T cell memory in response to different stimuli: cell population structure and protective function. *Immunol. Cell Biol.*, 79:74–86, 2001.
- [9] A. Ciurea, P. Klenerman, L. Hunziker, E. Horvath, B. Odermatt, A. F. Ochsenbein, H. Hengartner, and R. M. Zinkernagel. Persistence of lymphocytic choriomeningitis virus at very low levels in immune mice. *Proc. Natl. Acad. Sci. USA*, 96:11964–11969, 1999.
- [10] P. C. Doherty. The numbers game for virus-specific CD8⁺ T cells. *Nature*, 280:227, 1998.
- [11] P. C. Doherty and J. P. Christensen. Accessing complexity: The dynamics of virus-specific T cell responses. *Annu. Rev. Immunol.*, 18:561–592, 2000.
- [12] P. C. Doherty, D. J. Topham, and R. A. Tripp. Establishment and persistence of virus-specific CD4⁺ and CD8⁺ T cell memory. *Immunol. Rev.*, 150:23–44, 1996.
- [13] S. Ehl, P. Klenerman, P. Aichele, H. Hengartner, and R. M. Zinkernagel. A functional and kinetic comparison of antiviral effector and memory CTL populations in vivo and in vitro. *Eur. J. Immunol.*, 27:3404–3413, 1997.
- [14] S. Ehl, P. Klenerman, R. M. Zinkernagel, and G. Bocharov. The impact of variation in the number of CD8⁺ T-cell precursors on the outcome of virus infection. *Cellular Immunology*, 189:67–73, 1998.

- [15] K. Engelborghs. *DDE-BIFTOOL: a Matlab package for bifurcation analysis of delay differential equations*. Department of Computer Science, Katholieke Universiteit Leuven, Belgium, March 2000. Report TW 305, (<http://www.cs.kuleuven.ac.be/~koen/delay/ddebiftool.shtml>).
- [16] K. Engelborghs. *Numerical bifurcation analysis of delay differential equations*. Ph.D. thesis, Department of Computer Science, Katholieke Universiteit Leuven, Belgium, 2000.
- [17] K. Engelborghs and E. J. Doedel. Stability of piecewise polynomial collocation methods for computing periodic solutions of delay differential equations. *Numer. Math.*, 2001. Accepted.
- [18] K. Engelborghs, T. Luzyanina, K. in't Hout, and D. Roose. Collocation methods for the computation of periodic solutions of delay differential equations. *SIAM J. Sci. Comput.*, 22:1593–1609, 2000.
- [19] K. Engelborghs and D. Roose. On stability of LMS methods and characteristic roots of delay differential equations. Submitted, 2000.
- [20] D. L. Farber. T cell memory: heterogeneity and mechanisms. *Clin. Immunol.*, 95:173–181, 2000.
- [21] A. A. Freitas and B. Rocha. Population biology of lymphocytes: The flight for survival. *Ann. Rev. Immunol.*, 18:83–111, 2000.
- [22] C. K. Hansen. *The role of antigen in immune responses. A bioinformatics approach*. Ph.D. thesis, Department of Biochemistry and Nutrition, Technical University of Denmark, and Theoretical Biology and Bioinformatics Group, Utrecht University, 1999.
- [23] M. G. Herrath, M. Yokoyama, J. Dockter, M. B. A. Oldstone, and J. L. Whitton. CD4-deficient mice have reduced levels of memory cytotoxic T lymphocytes after immunization and show diminished resistance to subsequent virus challenge. *J. Virol.*, 70:1072–1079, 1996.
- [24] P. Klenerman, H. Hengartner, and R. M. Zinkernagel. A non-retroviral RNA virus persists in DNA form. *Nature*, 390:298–301, 1997.
- [25] P. Klenerman and R. M. Zinkernagel. What can we learn about human immunodeficiency virus from a study of lymphocytic choriomeningitis virus? *Immunol. Rev.*, 159:5–16, 1997.
- [26] T. M. Kündig, M. F. Bachman, H. Pircher, P. Ohashi, H. Hengartner, and R. M. Zinkernagel. On T cell memory: arguments for antigen dependence. *Immunol. Rev.*, 150:63–90, 1996.
- [27] F. Lehmann-Grube. *Lymphocytic Choriomeningitis Virus*. New York:Springer-Verlag, 1971.
- [28] M. Lenardo, F. Ka-Ming Chan, F. Hornung, H. McFarland, R. Siegel, J. Wang, and L. Zheng. Mature T lymphocyte apoptosis - immune regulations in a dynamic and unpredictable antigenic environment. *Ann. Rev. Immunol.*, 17:221–253, 1999.

- [29] A. Levy, J. L. Mullins, and B. D. Walker. Cellular immune responses and viral diversity in individuals treated during acute and early HIV-1 infection. *J. Exp. Med.*, 193:169–180, 2001.
- [30] M. K. Maini and A. Bertoletti. How can the cellular immune response control hepatitis B virus replication? *J. Viral. Hepat.*, 7:321–326, 2000.
- [31] P. Marrack, J. Bender, D. Hildeman, M. Jordan, T. Mitchell, M. Murakami, A. Sakamoto, B. C. Schaefer, B. Swanson, and J. Kappler. Homeostasis of $\alpha\beta$ TCR⁺ T cells. *Nature Immunol.*, 1:107–111, 2000.
- [32] D. Moskophidis, M. Battegay, M. A. Bruendler, E. Laine, I. Gresser, and R. M. Zinkernagel. Resistance of lymphocytic choriomeningitis virus to alpha/beta interferon and to gamma interferon. *J. Virol.*, 68:1951–1955, 1994.
- [33] D. Moskophidis, F. Lecher, H. Pircher, and R. M. Zinkernagel. Virus persistence in acutely infected immunocompetent mice by exhaustion of antiviral cytotoxic effector T cells. *Nature*, 362:758–761, 1993.
- [34] A. Müllbacher. The long-term maintenance of cytotoxic T cell memory doesn't require persistence of antigen. *J. Exp. Med.*, 179:317–321, 1994.
- [35] K. Murali-Krishna, J. D. Altman, M. Suresh, D. J. Sourdive, A. J. Zajac, J. D. Miller, J. Slansky, and R. Ahmed. Counting antigen-specific CD8 T cells: a reevaluation of bystander activation during viral infection. *Immunity*, 8:177–187, 1998.
- [36] K. Murali-Krishna, L. L. Lau, S. Sambhara, F. Lemonnier, J. Altman, and R. Ahmed. Persistence of memory CD8 T cells in MHC class I-deficient mice. *Science*, 286:1377–1381, 1999.
- [37] M. A. Nowak and C. R. Bangham. Population dynamics of immune responses to persistent viruses. *Science*, 272:74–79, 1996.
- [38] A. F. Ochsenbein, U. Karrer, P. Klenerman, A. Althage, A. Ciurea, H. Shen, J. F. Miller, J. L. Whitton, H. Hengartner, and R. M. Zinkernagel. A comparison of T cell memory against the same antigen induced by virus versus intracellular bacteria. *Proc. Natl. Acad. Sci. USA*, 96:9293–9298, 1999.
- [39] S. Oehen, H. Waldner, T. Kündig, H. Hengartner, and R. M. Zinkernagel. Antivirally protective cytotoxic T cell memory to lymphocytic choriomeningitis virus is governed by persisting antigen. *J. Exp. Med.*, 176:1273–1281, 1992.
- [40] M. B. A. Oldstone. Viral persistence. *Cell*, 56:517–520, 1989.
- [41] M. Pihlgren, P. M. Dubos, M. Tomkowiak, T. Sjörgen, and J. Marvel. Resting memory CD8⁺ T cells are hyperreactive to antigenic challenge in vitro. *J. Exp. Med.*, 184:2141–2151, 1996.

- [42] O. Planz, S. Ehl, E. Furrer, E. Horvath, M.-A. Bründler, H. Hengartner, and R. M. Zinkernagel. A critical role of neutralizing-antibody-producing B cells, CD4⁺ T cells and interferons in persistent and acute infections of mice with lymphocytic choriomeningitis virus: Implications for adoptive immunotherapy of virus carriers. *Proc. Natl. Acad. Sci. USA*, 94:6874–6879, 1997.
- [43] H. L. Ploegh. Viral strategies of immune evasion. *Science*, 280:248–253, 1998.
- [44] B. Rehermann, C. Ferrari and C. Pasquinelli, and F.V. Chisari. The hepatitis B virus persists for decades after patients’ recovery from acute viral hepatitis despite active maintenance of a cytotoxic T-lymphocyte response. *Nat. Med.*, 2:1104–1108, 1996.
- [45] L. K. Selin and R. M. Welsh. Cytolytically active memory CTL present in lymphocytic choriomeningitis virus-immune mice after clearance of virus infection. *J. Immunol.*, 158:5366–5373, 1997.
- [46] J. Sprent and D. F. Tough. Lymphocyte life-spans and memory. *Science*, 265:1395–1400, 1994.
- [47] K. Takumi. *Evolutionary, network, and cellular memory in immune systems*. Ph.D. thesis, Theoretical Biology and Bioinformatics Group, Utrecht University, The Netherlands, 1998.
- [48] C. Tanchot, F. A. Lemonnier, B. Pérarnau, A. A. Freitas, and B. Rocha. Differential requirements for survival and proliferation of CD8 naive or memory T cells. *Science*, 276:2057–2062, 1997.
- [49] A. R. Thomsen, J. Johansen, O. Marker, and J. P. Christensen. Exhaustion of CTL memory and recrudescence of viremia in lymphocytic choriomeningitis virus-infected MHC class II-deficient mice and B cell-deficient mice. *J. Immunol.*, 157:3074–3080, 1996.
- [50] A. R. Thomsen, A. Nansen, S. O. Andreasen, D. Wodarz, and J. P. Christensen. Host factors influencing viral persistence. *Proc. R. Soc. Lond. B*, 355:1031–1041, 2000.
- [51] D. Tortorella, B. E. Gewurz, M. H. Furman, D. J. Schust, and H. L. Ploegh. Viral subversion of the immune system. *Ann. Rev. Immunol.*, 18:861–926, 2000.
- [52] D. F. Tough and J. Sprent. Turnover of naive- and memory-phenotype T cells. *J. Exp. Med.*, 179:1127–1135, 1994.
- [53] D. Wodarz, P. Klenerman, and M. Nowak. Dynamics of cytotoxic T-lymphocyte exhaustion. *Proc. R. Soc. B.*, 265:191–203, 1997.
- [54] A. J. Zajac, J. N. Blattman, K. Murali-Krishna, D. J. D. Sourdive, M. Suresh, J. D. Altman, and R. Ahmed. Viral immune evasion due to persistence of activated T cells without effector function. *J. Exp. Med.*, 188:2205–2213, 1998.
- [55] C. Zimmermann, K. Brduscha-Riem, C. Blaser, R. Zinkernagel, and H. Pircher. Visualization, characterization, and turnover of CD8⁺ memory T cells in virus-infected hosts. *J. Exp. Med.*, 183:1367–1375, 1996.

- [56] R. M. Zinkernagel. Immunology taught by viruses. *Science*, 271:173–178, 1996.
- [57] R. M. Zinkernagel. On immunological memory. *Phil. Trans. R. Soc. Lond. B*, 355:369–371, 2000.
- [58] R. M. Zinkernagel. What is missing in immunology to understand immunity? *Nature Immunol.*, 1:181–185, 2000.
- [59] R. M. Zinkernagel, H. Hengartner, and L. Stitz. On the role of viruses in the evolution of immune responses. *Brit. Med. Bull.*, 41:92–97, 1985.
- [60] R. M. Zinkernagel, D. Moskophidis, T. Künding, S. Oehen, H. Pircher, and H. Hengartner. Effector T-cell induction and T-cell memory versus peripheral deletion of T cells. *Immunol. Rev.*, 131:199–223, 1993.